Lecture 5. Energetics and Dynamics of Biological Systems

Membrane Transport and Membrane Potential

The living cell and its internal compartments maintain a particular electrolyte state which on the one hand guaranties constant conditions for all enzymatic processes, whilst on the other hand, it acts as an accumulator of electrochemical energy. This requires a complicated system of transporters in the membranes, which are particularly specialized and precisely controlled by a system of interactions. Furthermore, a number of receptor proteins transform external signals to internal information by modification of their transport properties. In a highly specialized way, nerve and muscle cells used the accumulated electrochemical energy for processes of excitation. In this chapter we will concentrate just on transport of ions with regard to transport of metabolites.

Numerous experimental investigations indicate an enormous variety of transporters even in a single cell. This research during the second half of the last century was supported strongly by the introduction of radioactive isotopes, later on by fluorometric methods and especially by the use of patch-clamp measurements. In the last decades, our knowledge on the molecular mechanisms of these transporters and their control has developed rapidly thanks to studies involving X-ray crystal analyses, and various high-resolution functional measurements.

Channels and Pumps: The Variety of Cellular Transport Mechanisms

Figure 3.25 illustrates a functional classification of various types of ion transport mechanisms in the membrane of cells and organelles. The differentiation between *pores* and *channels* is rather unclear. Mostly the term “pore” is used to denote larger membrane openings with low selectivity, which are for example produced by electric pulses (electric break down, see Sect. 3.5.5) or by other influences. In contrast “channels” are protein transporters, which are characterized by a certain selectivity. In any case, fluxes through these kinds of transporters are governed by the laws of electrodiffusion.

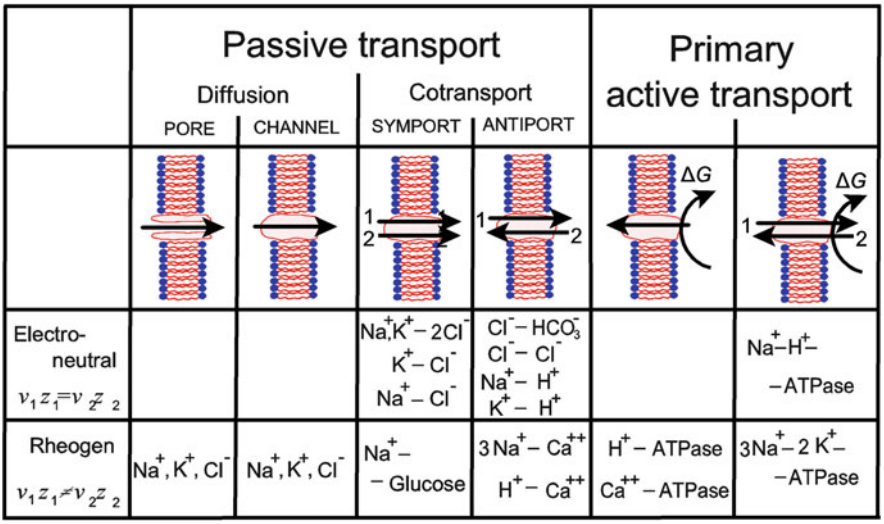

Fig. 3.25 Classification of various systems of ion transporters in biological membranes, including particular examples

Another type of passive transporters is so-called *carriers* or *porters* transporting simultaneously two or more ions in a well-defined stoichiometric relation. Such stoichiometrically coupled fluxes are called *co-transports*. There are two kinds of co-transport systems: In the case of the *symport,* a strongly coupled flux of two species in the same direction occurs. An example of this could be a complex that simultaneously transfers one Cl^- and one K^+ ion through the membrane in the same direction. In the same way, transport of an ion could be coupled to an uncharged molecule, like glucose. An *antiport*, in contrast to this, is a system simultaneously transporting two ions with identical charges in opposite directions, for example one K^+, against one H^+.

Co-transport systems are electroneutral, if an equal number of charges is transported, either of opposite sign in the case of a symport, or of the same sign in antiports. In this case the flux does not depend directly on electric field conditions. It is electrically silent, i.e., it cannot be identified by electrophysiological methods. In cases of unequal charge transporters, an electrical current will be the result of the transport. We will call this type of process *rheogenic*, i.e., "current producing." Rheogenic co-transport processes can be recognized by their electrical conductivity, a property which they have in common with simple diffusion processes. They can be controlled by electric fields, especially by the transmembrane potential.

An *active transport* is a sort of pump, transporting ions or even uncharged molecules against their own chemical or electrochemical gradients. Therefore, it is an "uphill transport," using metabolic energy (ΔG, in Fig. 3.25). In most cases these are so-called transport ATPases, using the energy of the hydrolytic reaction: ATP $\Rightarrow$ ADP. Furthermore, ionic pumps are known which are driven by other

sources of energy, such as for example decarboxylation, oxyreduction, or even the quantum energy of light. Some of these mechanisms can also run in the opposite direction. In chloroplasts and mitochondria, for example, ATP is synthesized by a "downhill" proton flux (see Sect. 4.8.3, Fig. 4.36).

Active transport can also be rheogenic. In this case the transport directly induces electric currents, like for example the Na-K-ATPase, transporting three charges from the inside out, but only two in the opposite direction, or a Ca^{++}-ATPase (see Sect. 3.5.2, Fig. 3.35). Frequently such transports are also called *electrogenic* which means: "generating an electrical membrane potential." Looking at the terms "rheogenic" and "electrogenic" accurately, they are however not identical. Even an electro-neutral pump can be "electrogenic" if it produces a concentration gradient of ions which subsequently generates a diffusion potential. Conversely, a rheogenic pump may influence the transmembrane potential only if there is a sufficiently high membrane resistance.

This leads to the differentiation between *primary* and *secondary* active transporters. An example of a primary active transporter is the Na-K-ATPase, where the uphill flux of ions is directly driven by a biochemical process. In contrast, secondary active transporters exploit the energy already stored in the electrochemical gradient of one species to drive the uphill transport of another substrate. This can be realized by various kinds of symporters or antiporters. As an example in Figs. 3.25 and 3.26 the co-transport of Na^+ with glucose is shown. It is "secondary active," because in fact the uphill glucose uptake is driven by the downhill Na^+-flux in a gradient, produced by the Na-K-ATPase. In a similar way fluxes of amino acids are coupled with transport of Na^+ or H^+ ions.

The number of different transport paths in a single membrane can be rather high. In Fig. 3.26 this is illustrated for the case of cells of a renal proximal tubule. It is

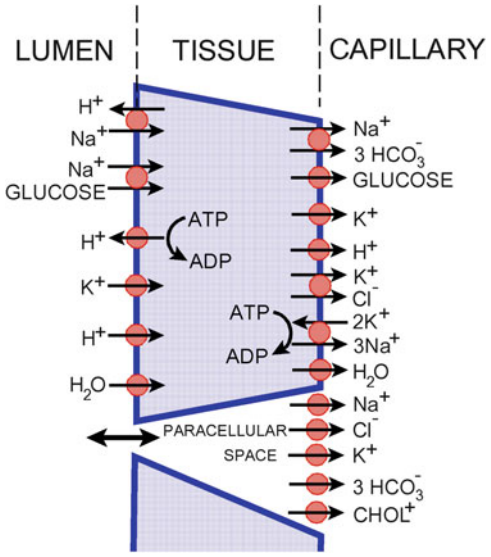

Fig. 3.26 Various types of ion transporters in cells of a renal proximal tubule and in the paracellular space (After Verkman and Alpern 1987)

obvious that the fluxes are coupled with each other by the transmembrane potential as well as by the concentrations of their common ions. Additionally, changes of fixed charges inside the cell induced by internal pH changes need to be taken into account.

The existence of transporters where the participants have strongly fixed stoichiometry forces us to rethink the requirement of flux electroneutrality which we postulated in Sect. 3.3.3 (Eq. 3.170). Considering rheogenic symports, it is not the electroneutrality of a single flux that is required, but rather the electroneutrality of all fluxes in the membrane of a single cell together. The calculation of the balance of charges and ions in a cell is therefore only possible by considering all fluxes. This type of coupling can formally be calculated using the flux matrix as discussed in Sect. 3.1.3.

The existence of co-transporters in a cell rather than simple diffusion processes can be regarded as a form of optimization. Ionic transport, based on electrodiffusion, strongly depends on the transmembrane potential. An alteration of the transmembrane potential would cause an immediate change of electrolyte fluxes in the whole cell, and subsequently a shift in the internal concentration of all ions. In contrast, the system of electroneutral co-transporters is independent of the transmembrane potential and will protect the cell against such disturbances.

Further Reading

Läuger 1991; Luckey 2008.

3.4.2 The Network of Cellular Transporters

If a cell were only a poly-electrolyte system without metabolically driven ion pumps it would remain in a state of Donnan equilibrium. This means that there would be a Donnan distribution of all mobile ions according to fixed charges, and as a result, a Donnan osmotic pressure (see Sects. 3.2.4, 3.2.5). In the living cell however, active transport systems driven by metabolic energy (Fig. 3.25) modify this ionic composition, as shown schematically in the model of Fig. 3.4b. The living cell therefore reaches a steady state, i.e., a stationary state of nonequilibrium in general (see Fig. 3.6), and for particular ionic species.

This nonequilibrium state has manifold functions. In general the cell can be regarded as a kind of electrochemical energy store which may be easily tapped. This, for example, is the case in electrical membrane de- and repolarizations (see Sect. 3.4.4). Furthermore, the nonequilibrium state of a system is the precondition for its homeostatic regulation. This, by the way, is also the reason for the increased temperature in homeothermic animals. The setting up of a concentration gradient of ions across the membrane makes the cells able to control and regulate an intracellular environment, which is the precondition of various cellular processes. In the case of Ca-ATPase an effective signal system is established. This pump creates an extremely low calcium level in the cytoplasm which is of the order of 10^4 times lower than the concentration in the extracellular fluid. In this way an important

signal transduction pathway is established, which can be triggered even by a minimal increase in the Ca-permeability of the membrane. The cytoplasmic Ca^{++}-ions act as a second messenger, in a number of cellular functions.

What therefore are the immediate effects of ionic pumps on the cell?

- They control and regulate the internal ionic milieu. In this way, steep gradients of the electrochemical potentials of particular ions are built up, essentially without changing the total internal ionic concentration. The internal potassium concentration of animal cells, for example, is usually much higher than the external one. Simultaneously however, the sodium concentration is lower to the same degree. The sum of both of these ions in the cytoplasm, taken together, is nearly the same as in the external medium.
- In the case of rheogenic pumps, they directly induce transmembrane potentials. In this case the pumps are called electrogenic.
- They can produce a direct osmotic effect changing the concentration of osmotically active substances.
- They can establish particular internal ionic conditions, controlling, for example, the extremely low intracellular calcium concentration.

Some direct consequences of the active transport processes can be demonstrated by the effects of stopping the pump through the use of specific inhibitors. In this case effects can be observed like Donnan-osmotic swelling, internal pH shifts, an increase in the internal calcium concentration, a change of transmembrane potential, etc. Mostly, using such inhibitors, the overall internal ionic conditions are altered.

As an example, the system of transport processes in kidney tubule cells is illustrated in Fig. 3.24. There are 13 different transport systems shown which determine the cellular milieu and additionally five other fluxes between the luminal and serosal surfaces of the epithelium across the paracellular gap. This picture in fact is incomplete as, for example, Ca^{++} fluxes are not shown, and the diagram does not include the intracellular organelles with their own transporters.

Using this example we will illustrate the interconnections of these transport properties qualitatively, following for example one particular path: Transport ATPases pump protons out of the cell, others decrease the internal sodium content, and in the same way enrich the cytoplasm with potassium. Extruding positive charges, both primary active transporters induce an inside negative transmembrane potential. Simultaneously, an electrochemical sodium gradient was generated which drives a sodium flux outside–in. This influx, however, is realized by a glucose-sodium co-transporter and acts therefore as a secondary active transporter for glucose entry. The glucose finally diffuses via its own concentration gradient on the opposite side of the cell layer from the cytoplasm into the capillary.

All these manifold transporters occurring in a single cell respond to different stimulants. Some of them become active only if a particular pH exists, others if the internal calcium concentration was increased. There are voltage-sensitive transporters responding to particular transmembrane potentials, or others that respond to mechanical stress of the membrane or to minimal temperature changes

(see Sect. 4.1). The electroneutral Na^+H^+ antiporter, which is present in most animal cells, merits particular attention. Under physiological conditions, at neutral pH_i it is inactive. However, if the internal pH increases, it becomes activated. This property qualifies it to be a volume-regulating system. This mechanism was demonstrated in the case of lymphocytes. It has also been shown that this Na^+ H^+ antiporter can be activated by a multitude of substances including hormones, growth factors, lectins, etc. These substances alter the above-mentioned pH threshold. This seems to be an important control mechanism for the regulation of complex biological phenomena.

Beside direct calculations of flux coupling, the equations of nonequilibrium thermodynamics can be applied to describe the energy balance of primary and secondary active transport. As an example the energy balance at steady state of the above-mentioned Na^+-Glucose symport will be evaluated. This is an example of a steady-state system like that of Fig. 3.4b which is determined by the active transport ($\mathbf{J}_A$) as well as by the passive flux ($\mathbf{J}_i$). In Sect. 3.1.4 we introduced the dissipation function $\mathbf{\Phi} = \sigma T$ (Eq. 3.64), which must be larger than 0. According to Eq. 3.64 for our system it amounts to

$$\Phi = \mathbf{J}_A\mathbf{X}_A + \mathbf{J}_i\mathbf{X}_i \quad \text{for:} \quad \Phi > 0 \tag{3.180}$$

In our particular case the glucose uptake ($\mathbf{J}_G$) is driven by the passive influx of sodium ($\mathbf{J}_{Na}$), driven by its electrochemical gradient. Corresponding to Eq. 3.180 this results in:

$$\mathbf{J}_G\mathbf{X}_G + \mathbf{J}_{Na}\mathbf{X}_{Na} > 0 \tag{3.181}$$

If v equivalents of sodium ions are transported for each mole of glucose then:

$$\mathbf{J}_G = v\mathbf{J}_{Na} \tag{3.182}$$

Introducing this in Eq. 3.181 and considering that both fluxes are not equal to zero, it follows that:

$$v\mathbf{X}_G + \mathbf{X}_{Na} > 0 \tag{3.183}$$

respectively:

$$\mathbf{X}_{Na} > -v\mathbf{X}_G \tag{3.184}$$

Let us now replace the forces ($\mathbf{X}$) by the differences of the corresponding chemical, resp. electrochemical potential (see Sect. 3.3.1), we obtain:

$$-v\Delta\mu_G < \Delta\tilde{\mu}_{Na} \tag{3.185}$$

Using Eqs. 3.33 and 3.41, and the conditions: $\Delta T = 0$ and $\Delta p = 0$, we get:

$$\nu \mathrm{R}T \ln \frac{a^i_{\mathrm{G}}}{a^e_{\mathrm{G}}} < -\left(\mathrm{R}T \ln \frac{a^i_{\mathrm{Na}}}{a^e_{\mathrm{Na}}} + \mathrm{F}\Delta\psi\right) \tag{3.186}$$

(where $\Delta\psi = \psi_i - \psi_e$) and after rearrangement:

$$\left(\frac{a^i_{\mathrm{G}}}{a^e_{\mathrm{G}}}\right)^{\nu} < \frac{a^e_{\mathrm{Na}}}{a^i_{\mathrm{Na}}} \quad \mathrm{e}^{-\frac{\mathrm{F}\Delta\psi}{\mathrm{R}T}} \tag{3.187}$$

This equation allows us to calculate the maximal rate of enrichment of glucose in the cell that can be achieved for a given electrochemical gradient of sodium ions. Assuming that the membrane potential of the cell is: $\Delta\psi = -50$ mV, and the relation of sodium ions: $a_{\mathrm{Na}}{}^{\mathrm{i}}/a_{\mathrm{Na}}{}^{\mathrm{e}} = 10$ ($T = 300$ K), it follows:

$$\left(\frac{a^i_{\mathrm{G}}}{a^e_{\mathrm{G}}}\right)^{\nu} < 69 \tag{3.188}$$

If the fluxes are coupled 1:1 ($\nu = 1$), this process gives a maximum enrichment of glucose by a factor of 69, when the pump is performing optimally.

Similar calculations can be applied to primary active transports, i.e., those that are driven by chemical reactions, for example transport ATPases. In this case in the equation of the dissipation function (Eq. 3.180), the reaction rate (as a type of scalar flux), and the chemical affinity of the energy supplying reaction (Eq. 3.75) must be included.

The calculation of the intensity of a pump which is necessary to build up a certain concentration gradient depends both on the coupling stoichiometry of the fluxes and on the passive back flow. This means that not only the power of the pump is responsible for the steady-state level achieved, but also the conductivity, resp. the permeability of the considered substance, leading it to flow backwards. This is illustrated in the scheme shown in Fig. 3.4b: the power of the pump must be higher if a greater difference in the levels of the vessels is reached, and if the outflow becomes faster.

Further Reading

Luckey 2008.

3.4.3 The Membrane Potential

As outlined in the previous section, the pumps lead to gradients of ion concentrations and therefore accumulate electrochemical energy. Now we will discuss how the cell generates an electrical membrane potential, using this accumulated energy.

First it is necessary to remember the general definition of electrical potential as defined in Sect. 2.2.1. According to this, the electrical potential [$\psi(x,y,z)$] is a scalar state parameter in three-dimensional space, similar to temperature (T) or pressure (p). Mostly as a simplification the function $\psi(x)$ is used to characterize the potential along a line that runs perpendicularly through the membrane (Figs. 2.15, 2.48). As the *transmembrane potential* ($\Delta\psi$) the potential difference is defined between two points, one on the inside, the other on the outside of the membrane, each at a suitable distance from it (Fig. 2.48). The sign of this difference results from its definition:

$$\Delta\psi = \psi_i - \psi_e \tag{3.189}$$

Note that terms such as Donnan potential, diffusion potential, Nernst potential, are just expressions describing the *mechanisms* which can give rise to the electrical transmembrane potential and do not refer in any way to different kinds of electrical potentials that might exist simultaneously. In fact there is only one electrical potential $\psi(x,y,z,t)$ at a given point in the space (x, y, z), and at a given time (t). In Fig. 2.48, the function $\psi(x)$ illustrates this in a very simplified way. It includes the transmembrane potential and the two surface potentials at both boundaries.

We have already learned that processes of active transport can be rheogenic (Fig. 3.25). If the so-far transported charges can be rapidly neutralized by other fluxes, for example by Cl^- exchange in the membrane of human erythrocytes, then a rheogenic pump has no direct electrical consequences for the cell. If however, no such short-circuit flux exists, the transported net charges build up a transmembrane potential, and the *rheogenic* pump becomes *electrogenic*.

In any case, the Na-K-ATPase, occurring in nearly all cell membranes, generates an electrochemical gradient of sodium and potassium. For most animal cells a relation near 1:10 occurs for $a^i_K > a^e_K$ and $a^i_{Na} < a^e_{Na}$. Chloride ions are distributed mostly passively, according to the Nernst equation. This nonequilibrium distribution of the cations can lead to a diffusion potential which can be calculated by the Goldman equation (Eq. 3.179) as follows:

$$\Delta\psi = \frac{RT}{F} \ln \frac{P_{Cl} a^i_{Cl} + P_K a^e_K + P_{Na} a^e_{Na}}{P_{Cl} a^e_{Cl} + P_K a^i_K + P_{Na} a^i_{Na}} \tag{3.190}$$

Even if the internal ion activities a^i_K and a^i_{Na} remain constant, the diffusion potential ($\Delta\psi$) can vary widely because of changing permeabilities (P_i). The limits of such variations can be easily obtained from Eq. 3.190:

For $P_K >> P_{Na}$, P_{Cl} Eq. 3.190 reduces to:

$$\Delta\psi_K = \frac{RT}{F} \ln \frac{a^e_K}{a^i_K} \tag{3.191}$$

and for $P_{Na} >> P_K$, P_{Cl} it follows:

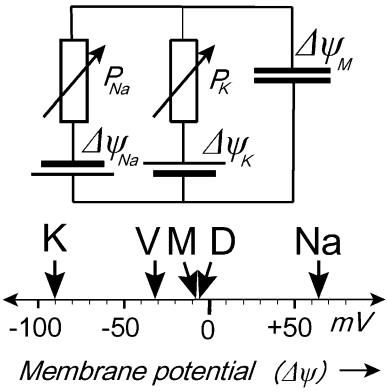

Fig. 3.27 An electrical circuit as a model illustrating the Na^+-K^+ diffusion potential of a cell as the result of a sodium ($\Delta\psi_{Na}$), and a potassium ($\Delta\psi_K$) battery. In the lower part of the figure, possible potential alterations are illustrated for the case of human erythrocytes in a solution containing 145 mM NaCl and 5 mM KCL. **K** – $\Delta\psi_K$, **V** – valinomycin-induced diffusion potential, **M** – potential of untreated erythrocytes corresponding to $\Delta\psi_M$, **D** – position of the Donnan potential, **Na** – $\Delta\psi_{Na}$

$$\Delta\psi_{Na} = \frac{RT}{F} \ln \frac{a^e_{Na}}{a^i_{Na}} \tag{3.192}$$

For these particular cases the Goldman equation (Eq. 3.190), therefore, reduces to a Nernst equation (Eq. 3.112) which was derived for such kinds of semipermeable membranes. If the typical relations of activities for sodium and potassium, as mentioned before, are inserted into Eqs. 3.191 and 3.192, then it is easy to understand that $\Delta\psi_K < 0$ and $\Delta\psi_{Na} > 0$.

This situation is illustrated in Fig. 3.27. The electrochemical gradients of potassium and sodium which are generated using metabolic energy can be considered as storage batteries, or electrical accumulators having opposite polarities. The permeability characteristics of the ions are expressed in this model as conductivities of the variable resistors, or potentiometers through which these accumulators are discharged. If the resistance is low, then a large discharge current would flow, and if the accumulator is not recharged continuously, it would soon be empty. In fact, the permeabilities P_{Na} and P_K are usually so low that the electrochemical gradient of the living cell persists for hours or even days. The effective membrane potential in this model is represented by the voltage difference across the capacitor $\Delta\psi_M$. This capacitor represents the capacity of the membrane (see Sect. 2.3.6). If P_{Na} and P_K have about the same value, then $\Delta\psi_M$ will be very small. If they differ, a membrane potential will be established according to Eqs. 3.191 and 3.192.

Figure 3.27 demonstrates membrane potentials that can be induced in human erythrocytes. In this case the Nernst potentials for potassium and sodium give the limits of these possible shifts. They range approximately between −95 mV and

+65 mV. The actual membrane potential of human erythrocytes in vivo is found to be −9 mV (**M**), and is only a little greater than the Donnan potential (**D**) which would result if the cell achieved a thermodynamic equilibrium (see Fig. 3.19). If the cells are treated with valinomycin, the membrane potential falls to about −35 mV (**V**). Valinomycin is an ionophore that is rapidly incorporated into the membrane causing a highly selective increase of potassium permeability. It will not reach the limiting value of the Nernst potential of potassium, because the values of P_{Cl} and P_{Na} are not negligible, as was assumed for Eq. 3.191. However, it is shifted in this direction.

Even if these types of potential alterations are possible without a significant change of concentration profiles, they must in fact be accompanied by a certain transmembrane shift of charges. It is easy to show that this charge flux is extremely small. For this we calculate the charge transfer across the membrane capacitor, which is required to adjust these potential differences ($\Delta\psi_M$ in Fig. 3.27). Let us ask the question: how many charges must be displaced in the cell membrane with a specific capacity of 10^{-2} F m^{-2} (see Sect. 2.3.6) in order to generate a transmembrane potential $\Delta\psi_M = 0.1$ V?

Equation 2.90 gives the corresponding relation for a capacitor. This enables us to calculate the surface charge density (σ) as a function of the transmembrane potential ($\Delta\psi$) and specific capacity (C_{sp}):

$$\sigma = C_{sp}\Delta\psi = 10^{-3}\text{C m}^{-2} \tag{3.193}$$

This value can be converted into charge equivalents of ions, using the Faraday constant (F):

$$\frac{\sigma}{\text{F}} = \frac{10^{-3}}{9.65 \cdot 10^4} \approx 10^{-8} \quad \text{charge equivalents} \cdot \text{m}^{-2}$$

The resulting charge density, so far, is very small. Considering a certain geometry of the cell, for example a sphere, or in the case of a neuron, a cylinder, one can easily transform this number into a concentration shift. The result will be a fully negligible proportion of the amount of internal ions.

This example demonstrates a most important element in the functional arrangement of the living cell: An ion pump driven by metabolic energy, accumulates electrochemical energy by generating a concentration gradient of sodium and potassium. This electrochemical energy can be converted into electrical energy altering the membrane permeabilities (for example: P_K and P_{Na}). In this way a wide-ranging control of the electric field in the cell membrane is possible. Even if the shift of the membrane potential amounts to only some tenths of a millivolt, the resulting variations of the field strength, sensed by the membrane proteins, are of the order of millions of volts per meter (see Sect. 2.2.1)! It must be emphasized that this control is possible without any sizeable input of energy and can be realized in milliseconds. Such permeability changes can be induced by the cell itself as well as by external influences.

As mentioned before, there are many ion-selective transporters in the cell which are controlled by internal calcium concentration, by internal pH, by mechanical tension of the membrane, or by modifications of other parameters. Diffusion potentials may also result from an interaction between the cell and specific drugs, or may be triggered locally through mechanical contacts with surfaces or particles, such as for example viruses. These alterations of membrane potentials caused by local permeability changes can induce electric potential differences and therefore electric fields not only in the x-direction, perpendicular to the membrane surface, but also in the y-, z-direction, i.e., in the plane of the membrane (see Sect. 3.5.2).

In the next section we will consider the action potential of nerve cells as a classical example of the feedback loop between an electric field and ionic permeability in more detail. Recently, the interest in the transmembrane potential of the cell as a regulator of cellular events has greatly increased. This concerns the size of the membrane potential in various cells, as well as its time dependence. Although action potentials have a special significance in signal transfer of neurons, they occur also in many other cells.

Although opening to particular transporters or integration of specific channels in the membrane may always modify the membrane potential by generating diffusion potentials, the resting potential of many cells is exclusively generated by electrogenic pumps. In this case transmembrane potentials appear to be independent of external potassium concentrations. Inhibition of the pumps in this case immediately leads to changes of $\Delta\psi$ (see Bashford and Pasternak 1986).

In Fig. 3.28 correlations of membrane potential and the state of various animal cells are illustrated. In contrast to cells with active proliferation like cancer cells or cells of embryos, indicating a transmembrane potential between -10 and -30 mV, nondividing cells, like neurons or skeletal muscle cells show membrane potentials between -70 and 90 mV. The transmembrane potential of cells which pass through a state of proliferation falls before mitosis takes place. It is not yet clear whether this reflects a regulatory mechanism of the cell, or whether it is only a phenomenon that accompanies such a mechanism.

In fact, in many cases alterations in the electrical field of a membrane seem to be of functional importance. The following mechanisms may cause this:

- The transverse component of an electrical field in the membrane may affect the functional state of intrinsic molecules. Dipole orientations for example, may modify the function of transport or other functional proteins, phase transitions in the lipid components of the membrane can be influenced by the field, or a transversal shift of small charged molecules can occur.
- The lateral component of the field can cause a displacement in its mosaic structure. This could lead to a local change in the mechanical properties of the membrane causing vesiculation, spike formation, etc.
- The electrical field can influence local ionic concentrations, as well as local pH values in close proximity to the membrane which, in turn, could affect transport processes, biochemical reactions at the membrane surface as well as receptor properties.

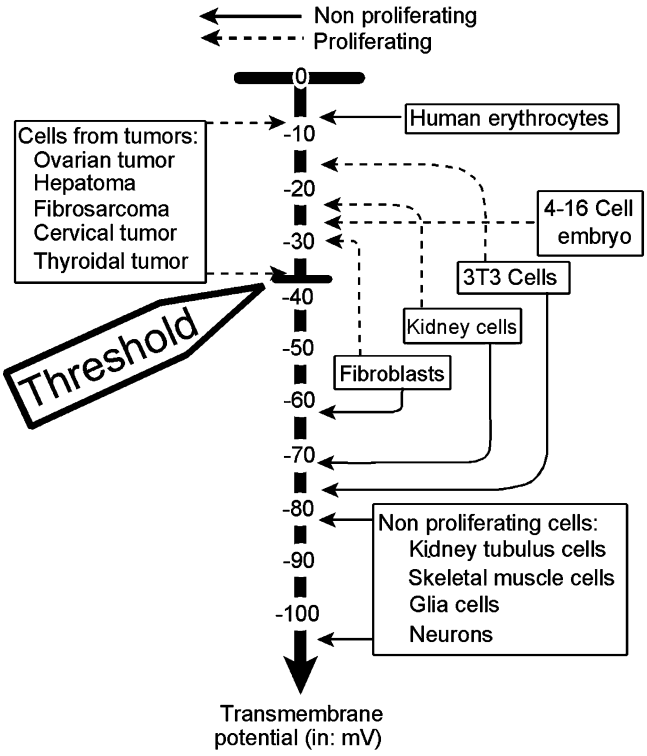

Fig. 3.28 The transmembrane potential of normal animal cells (*right*) and transformed tumor cells (*left*). It can be seen that proliferating cells indicate a membrane potential which is above the threshold value of −37 mV. Cells transiently arriving at the proliferating state lower their absolute potential. The human erythrocyte, as a non-nucleated cell with special physiological functions appears to be an exception (Drawn according to values from Bingeli and Weinstein 1986)

Further Reading

Glaser 1996; Starke-Peterkovic et al. 2005; Wang et al. 2003.

3.4.4 The Action Potential

In the previous section we described the possibility of cells to use the electrochemical gradient of potassium and sodium ions which is built up by active transport, to trigger various amounts of membrane potential simply by changing their permeabilities. This mechanism is expressed most efficiently in nerve and muscle cells. This was the reason why excitation phenomena were detected first in these cells.

Particular progress was achieved following the rediscovery of the giant axon of the squid in 1937 by John Zachary Young, and its subsequent introduction for biophysical measurements by Kenneth Stewart Cole. The use of these giant axons

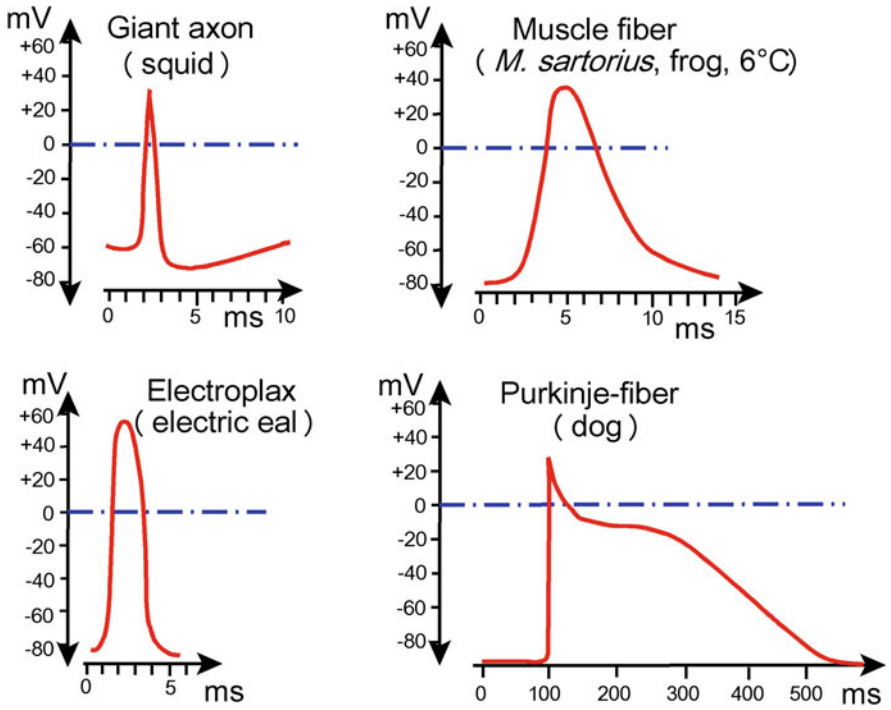

Fig. 3.29 Examples of various action potentials (After Penzlin 1991)

with a diameter up to 1 mm, have made it possible to apply the voltage-clamp technique to determine the ionic currents during the nerve impulse in extensive experiments by Alan Lloyd Hodgkin and Sir Andrew Fielding Huxley. In this technique, the electrical conductivity of the membrane is determined at various fixed transmembrane potentials, generated by microelectrodes. Recently, using patch-clamp techniques it has been possible to investigate the kinetics of these permeability alterations in extremely small membrane areas.

The action potentials of various nerve and muscle cells as illustrated in Fig. 3.29, can be qualitatively explained using the electrical scheme of Fig. 3.27 which was discussed in the previous section. The nonexcited nerve shows a very low sodium permeability (P_{Na}), its resting potential therefore, was determined chiefly by the diffusion potential of potassium which is negative inside-out. After excitation the membrane permeability for ions increased abruptly, whereas the sodium permeability rose quicker than that of potassium. For a short time therefore, the diffusion potential of sodium becomes dominant. This has the opposite polarity to the potassium potential which explains the spike of the action potentials.

As we demonstrated in the previous section the amount of charges that are needed for this kind of depolarization is extremely low. This was checked by flux measurements in excited nerves. During the generation of an action potential, therefore, no significant alterations of the internal ion concentration occur.

A nerve can generate action potentials for a long time after the ion pumps have been blocked. Only after hours does the electrochemical battery of the cell become empty.

Beside the entire mechanism of membrane excitation, the translation of the action potential along the axon of a nerve cell is of particular interest. In unmyelinated axons the process of pulse transmission is based on a lateral spreading of excitability by the electric field, generated by the excitation itself (see Fig. 3.37). The action potential generated by excited proteins in the membrane triggers the behavior of neighboring proteins. The impulse can proceed only in one direction, because of the refractory period of several milliseconds which the proteins need after an excitation to become excitable again.

Figure 3.30 illustrates the advantage of this kind of impulse propagation in relation to the transmission of a voltage pulse in an electric cable. In contrast to the cable, the time characteristics of the nerve pulse remains more or less constant, even after a certain distance of transmission. Conversely of course, the absolute velocity of pulse transmission in a cable is much faster than in an axon of a nerve.

The advantage of simple electrical conductivity is used in many vertebrate, and in a few invertebrate axons. In this case the axons are surrounded by *Schwann cells* forming the myelin sheath as an electrically isolating layer. Such nerves are called *myelinated*. This sheath is interrupted at intervals of some millimeters by so-called *nodes of Ranvier*, i.e., unmyelinated regions. In the myelinated regions simple electric conductivity of the pulse occurs, as in a cable. The nodes of Ranvier represent membrane areas which are excitable in a normal way. If a certain node of Ranvier is excited, then the pulse propagates by simple electric conduction along the myelinated length and excites the subsequent node. This so-called *saltatory conduction* is a form of pulse amplification leading to a faster transport of information. In contrast to about 1 m/s in unmyelinated nerves, the pulse propagation in fast myelinated nerves is up to 100 m/s.

In 1952 Hodgkin and Huxley, based on intensive experimental investigations on squid axons, proposed a theoretical model of membrane excitation in nerves (Nobel Prize 1963). Its form is of a purely kinetic nature and does not contain information about concrete molecular mechanisms taking place in the membrane.

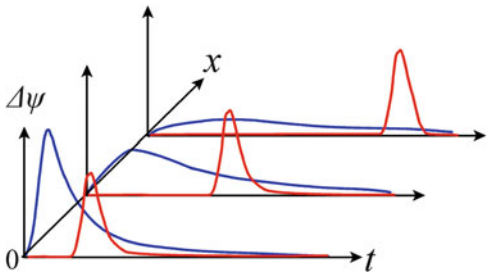

Fig. 3.30 The time course of a voltage pulse which is set at time $t = 0$ at point $x = 0$, transmitted in an isolated cable (*blue lines*) and in an unmyelinated nerve (*red lines*)

The basic equation describes the kinetics of the current in an electrical circuit, similar to the scheme in Fig. 3.27. The current density (j) in such a system can be described by the following equation:

$$j = C' \frac{\mathrm{d}(\Delta\psi_\mathrm{M})}{\mathrm{d}t} + (\Delta\psi_\mathrm{M} - \Delta\psi_\mathrm{K})G'_\mathrm{K} + (\Delta\psi_\mathrm{M} - \Delta\psi_\mathrm{Na})G'_\mathrm{Na} \tag{3.194}$$

$\Delta\psi_M$ is the electrical membrane potential, whereas the symbols $\Delta\psi_\mathrm{K}$ and $\Delta\psi_\mathrm{Na}$ indicate the Nernst potentials of potassium and sodium according to Eqs. 3.191 and 3.192. C' is the capacity of the membrane, and $G_\mathrm{K}{}'$ and $G_\mathrm{Na}{}'$ the potassium and sodium conductivities, always corresponding to a unit of area in the membrane. The conductivity of the membrane for individual ions cannot be measured electrically but can be obtained from experiments in which the kinetics of radioactive tracer ions is measured.

The first term of Eq. 3.194 gives the current density which leads to the charge of the membrane capacitor (Fig. 3.27). The following terms represent the current densities associated with potassium and sodium fluxes.

The conductivities $G_\mathrm{K}{}'$ and $G_\mathrm{Na}{}'$ are not constant, but functions of the electric field in the membrane, resp. of the membrane potential. The potentiometers in Fig. 3.27, therefore, are controlled directly by $\Delta\psi_M$. From the molecular point of view this means that these conductivities are the result of voltage-dependent channels. It is therefore necessary to make statements about field dependents of these conductivities, i.e., the functions $G_\mathrm{K}{}'(\Delta\psi_M)$ and $G_\mathrm{Na}{}'(\Delta\psi_M)$.

To describe the behavior of these channels, Hodgkin and Huxley used a statistical approach. They assumed that the channels can obtain only two discrete states: "open," or "closed." The phenomenological conductivities ($G_\mathrm{K}{}'$, $G_\mathrm{Na}{}'$) then represent the average of the functional states of a large number of such channels. If all of the channels are open then the maximal conductivities $G'_{\mathrm{K\ max}}$ and $G'_{\mathrm{Na\ max}}$ are established.

Furthermore, it is assumed that the potassium channel will be open when exactly four events take place simultaneously, all having the same probability of occurrence (n). The real nature of these events is not explained. It could be, for example, the presence of four potassium ions near the entrance of the channel.

This assumption leads to the following equation:

$$G'_\mathrm{K} = G_{\mathrm{K\ max}} n^4 \tag{3.195}$$

The probability n is a function of time and can be characterized by rate constants α_n and β_n as follows:

$$\frac{\mathrm{d}n}{\mathrm{d}t} = \alpha_\mathrm{n}(1 - n) - \beta_\mathrm{n} n \tag{3.196}$$

Concerning the sodium permeability, it is assumed that the channel will be open when three events, each having the probability m occur simultaneously, and if

another inhibitory event having the probability h has not taken place. This leads to the expression

$$G'_{\mathrm{Na}} = G_{\mathrm{Na\,max}} m^3 h \tag{3.197}$$

For the parameters m and h also kinetic equations can be written:

$$\frac{\mathrm{d}m}{\mathrm{d}t} = \alpha_{\mathrm{m}}(1-m) - \beta_{\mathrm{m}} m \tag{3.198}$$

$$\frac{\mathrm{d}h}{\mathrm{d}t} = \alpha_{\mathrm{h}}(1-h) - \beta_{\mathrm{h}} h \tag{3.199}$$

The voltage dependence of the channels is proposed to be the result of influences on the rate constants α and β:

$$\alpha_{\mathrm{n}} = \frac{0{,}01(\Delta\psi+10)}{\mathrm{e}^{\frac{\Delta\psi+10}{10}}-1} \quad \beta_{\mathrm{n}} = 0{,}125\ \mathrm{e}^{\frac{\Delta\psi}{80}}$$

$$\alpha_{\mathrm{m}} = \frac{0{,}1(\Delta\psi+25)}{\mathrm{e}^{\frac{\Delta\psi+25}{10}}-1} \quad \beta_{\mathrm{m}} = 4\ \mathrm{e}^{\frac{\Delta\psi}{18}}$$

$$\alpha_{\mathrm{h}} = 0{,}7\mathrm{e}^{\frac{\Delta\psi}{20}} \quad \beta_{\mathrm{h}} = \frac{1}{\mathrm{e}^{\frac{\Delta\psi+30}{10}}+1} \tag{3.200}$$

(In these equations, the potentials are in mV!)

These equations were obtained from a purely empirical approach, analyzing measured parameters.

It is easy to see that if the relations given in Eq. 3.200 are substituted into Eqs. 3.196, 3.198, and 3.199, a system of nonlinear differential equations will be obtained. The solution of these equations can be substituted into Eqs. 3.195 and 3.197, and eventually, into the basic Eq. 3.194. An analytical solution of this system of differential equations is not possible. Computer simulations of these equations, however, indicate a good accordance with experimental results.

Figure 3.31 shows the calculated time courses for the changes in sodium and potassium conductivities at different membrane potentials. This also corresponds well with experimental findings. These curves illustrate the mechanism described above for the generation of an action potential. The conductivities from Fig. 3.31 illustrate the time-dependent changes of the potentiometers shown in Fig. 3.27, whereas the conductivities are directly proportional to the permeabilities. Within the first millisecond following the stimulus, the sodium potential is dominant because of the rapid increase in $G_{\mathrm{Na}}{}'$ (and thus P_{Na}). This will then be counteracted, by the increasing potassium potential.

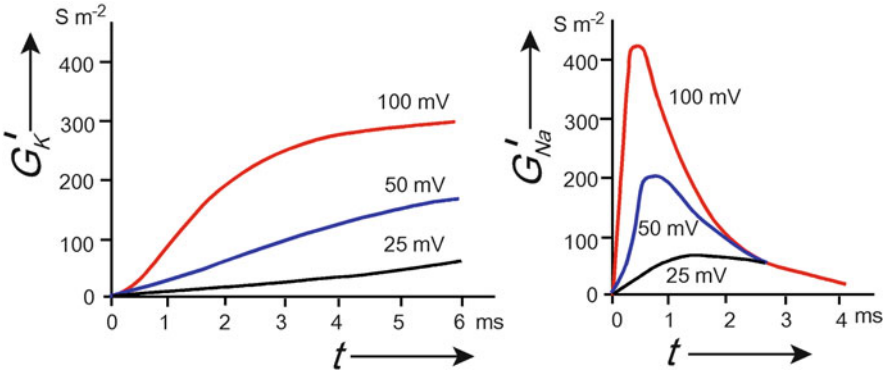

Fig. 3.31 The time dependence of the conductivities G_K' and G_{Na}' for various membrane potentials, corresponding to the theory of Hodgkin and Huxley

The Hodgkin–Huxley model and the corresponding measurements have provided a benchmark in our understanding of cellular excitability. New experimental techniques leading to more precise data nevertheless require some revisions of these approaches. So for example the mechanisms for the voltage-gated potassium and sodium ion currents have been superseded by more recent formulations that more accurately describe voltage-clamp measurements of these components. Especially its current–voltage relation has a nonlinear dependence upon driving force, corresponding to the Goldman–Hodgkin–Katz relation, rather than the linear approach used by Hodgkin and Huxley.

The original formulations of G'_{Na} and G'_K by Hodgkin and Huxley nevertheless continue to be used even though they do not adequately fit voltage-clamp measurements. The deviations between the m^3h and n^4 models (Eqs. 3.195 and 3.197), and the corresponding sodium and potassium currents do not appear to be eminently significant. Models that do describe these circumstances more precisely are more complex, which limits their practical utility in computational neuroscience.

Further Reading

Clay 2005; Hodgkin and Huxley 1952; Huxley 2002.

3.4.5 Molecular Aspects of Membrane Transport

In Sect. 3.4.1 various types of membrane transporters were characterized only in a phenomenological way. Now we will direct our attention to their structure and function. In fact, charged hydrophilic ions and molecules can penetrate the lipid membrane of cells and organelles only with the help of these mediators, usually proteins, the polypeptide chains of which span the lipid bilayer several times. In the last decades the molecular structure of a large number of these proteins has been revealed thanks to X-ray crystallography. In this way, the former more or less

mechanistic models of transport processes were replaced by more realistic molecular mechanisms.

In general, the following properties of transporters require an answer from these molecular considerations:

- Their extremely high selectivity including the phenomena of dehydration and rehydration of hydrophilic species in the process of membrane permeation.
- The mechanism of coupling between transport and the energy supporting biochemical reactions.
- The mechanisms of transport regulation by ligands and the transmembrane potential.

In 1998 MacKinnon unlocked the three-dimensional molecular structure of a potassium channel, a success which was awarded with the Nobel Prize in 2003. Such K^+ channels are found in bacterial as well as in eukaryotic cells of plants and animals, which are related members of a single protein family. Their amino acid sequences are easy to recognize because they contain a highly conserved segment called the K^+ channel signature sequence.

Let us answer some of the questions noted above using this extensively investigated example. The pore of this transporter is comprised of four identical subunits that encircle the central ion conduction pathway (two of them are depicted in Fig. 3.32). Each subunit contains two fully transmembrane α-helices, and a tilted pore helix that runs half way through the membrane. The hydrated K^+ ion, entering this channel from the cytoplasmatic side, first remains in the hydration state in a water-filled cavity with a diameter of 1 nm near the midpoint of the membrane. This cavity helps the K^+-ion to overcome the electrostatic repulsion that it would

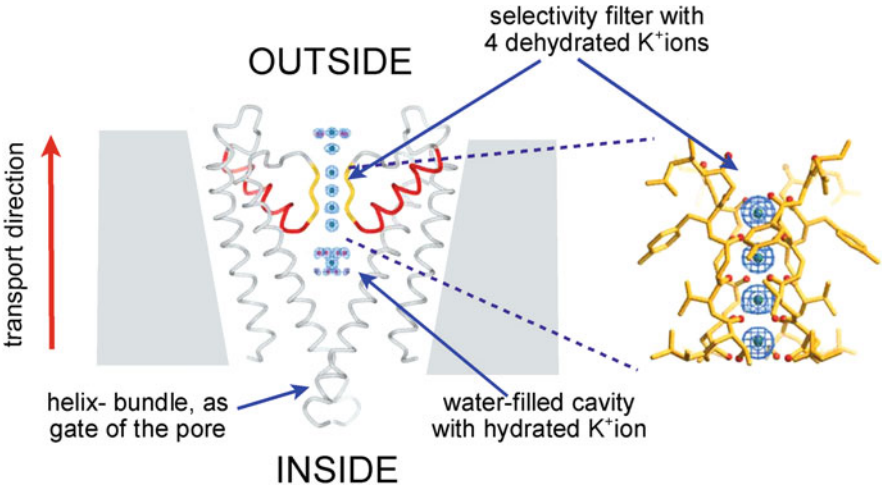

Fig. 3.32 The molecular structure of the KcsA channel. Only two subunits of this tetrameric molecule are shown. According to the position of the intracellular ends of the inner helices forming the gate, it is shown in a closed state (From MacKinnon 2003, modified)

normally experience when moving from the cytoplasmatic water phase into the low dielectric membrane environment. By allowing it to remain hydrated at the membrane center, and by directing the C-terminal negative ends of the protein helices toward the ion pathway, it becomes stabilized at the membrane interior. After this it enters the selectivity filter which contains four evenly spaced layers of carbonyl oxygen atoms, and a single layer of threonine hydroxyl oxygen atoms, which create four K^+ binding sites. In fact, on average only two K^+ ions are present at a given time in these four positions, always separated by one water molecule. It is very important that the arrangement of these protein oxygen atoms is very similar to that of water molecules around the hydrated K^+ ion. In this way the energetic cost of dehydration is minimized. Furthermore, a part of the binding energy is used for conformational changes of the proteins, which also is a prerequisite for the high conduction. In fact, the flux achieves up to 10^8 ions per second. This rate is large enough for sensitive amplifiers to record the electric current of a single channel. Na^+ ions cannot enter this filter because of their different crystal structure.

The gate of the channel is represented by a helix bundle near the intracellular membrane surface. In the closed position, as depicted in Fig. 3.32, the pore narrows to about 0.35 nm and is lined with hydrophobic amino acids, creating an effective barrier to the hydrophilic ions. This structure seems to be representative for many different potassium channels, irrespective of the stimulus that causes the pore to be in closed or open state. The conformational changes of these polypeptide chains that open and close the channel gate occur on the order of 10^2 times per second.

As discussed in previous chapters the membrane potential, and consequently the membrane electric field and its modification forms not only the basic principle of nerve and muscle excitation but regulates various functions in nearly all cells. This requires proteins, especially transporters, embedded in the membrane that sense alterations of this field and transform them into various cellular signals.

It is easy to imagine how an electric charge or an electric dipole can be reorientated within a protein when the field is changed. This can produce a conformational change in the protein that may regulate its function. The movement of the charge or the dipole induces a transient current (*gating current*) that can be measured experimentally and provides direct information about such conformational changes. The extent of the charge movement depends on the magnitude of the charge and the strength of the electric field in the region where the charge moves. In Sect. 2.2.1 (Fig. 2.15) as a crude estimation, this field strength was indicated to be of the order of 10^7 V m^{-1}. In fact, the exact value of this parameter near the corresponding charges or dipoles is unknown. In some cases the field can be concentrated to a narrow region around this location. Furthermore, the dielectric constant of this region inside the molecular structure is unknown.

The most extensively investigated voltage-gated channel is the so-called Shaker K^+ channel which can be expressed at a high density in *Xenopus* oocytes. It was isolated from *Drosophila melanogaster* and was named after the shaking that the fly

undergoes under anesthesia in its absence. Measurement of the gating current by patch-clamp techniques indicates that 13 electron equivalent charges per molecule are moving in this case. On the basis of the crystal structure of this protein, the so-called *paddle model* was proposed. It is assumed that voltage-gating charges are located on a hydrophobic helix-turn-helix structure, the so-called S4-segment, which can move within the membrane near the protein–lipid interface according to the direction of the electric field. Recently an S4-type sensor has been found in a voltage-dependent phosphatase, suggesting that this type of sensor may be modular and might have been incorporated into other types of proteins.

The kinetic model of nerve excitation as discussed in the previous section requires a particular sequence of opening and closing of potassium and sodium channels controlled by the membrane potential. Probably the four voltage-sensor domains of these channels react with individual time courses.

Although K^+ channels are excellent prototypes for voltage-gated channels, there are several other types of membrane proteins that differ in function, selectivity, regulation, kinetics, and voltage dependence. So for example a G-protein coupled muscarinic receptor has been found, in which a voltage-sensor is an integral part of the structure. It is expected that many other sensors will be discovered in the near future. More structures and biophysical analyses are still needed for a full molecular understanding of the function of these voltage sensors.

In contrast to the relatively simple mechanisms of channels, the pumps, and the co-transport systems require more functional elements, and the transport mechanisms demand more conformational changes in the corresponding transport protein. Especially the energy release by hydrolyzing ATP, and its coupling to ion movement needs a series of protein conformations. The first atomic-resolution structure of an ion pump was published in 2000 for the Ca-ATPase by Toyoshima et al. It shows an integral membrane protein with a large extended cytosolic part. In spite of the enormous progress of research in this field, a number of questions, especially concerning the Na-K-ATPase, are still open. The required conformational changes that accompany these transport processes mean that their speed is much slower than processes of channel transport.

The progress in determining the molecular structures of these channels has greatly facilitated the theoretical modeling and numerical simulation of the ion transport process itself. The most detailed description is based on the concept of *molecular dynamics* (MD). In this case microscopic forces of interactions between the penetrating ion and all atoms of the channel are calculated based on the classical Newton's equation of motion. This leads to trajectories of all the atoms in the system. In recent years, this approach has been used to simulate an increasing number of channels. Although this is the most detailed and accurate approach, it is limited by its shortcomings in quantitatively characterizing a large system, and its application depends considerably on advanced computational techniques.

Simpler and computationally less expensive of course are continuum models based on macroscopic or semimicroscopic continuum calculations like the Poisson–Nernst–Planck (PNP) approach. They, however, include a number of